Electronic Supplementary Material (ESI) for New Journal of Chemistry.

Magnetically Separable Ag@Fe_3O_4-GO Nanocomposites for SERS Detection, Removal of Organic Pollutants, Oil from Water, and Antibacterial Applications

Keshav Sharma[a], Shukla Majhi[a], Renuka Singh[a] Surbhi Sharma[a], Priya Dhyani[c], Chhaya Goyal[c], Chandra Shekhar Pati Tripathi*[b] and Debanjan Guin*[a]

[a] Department of Chemistry, Institute of Science, Banaras Hindu University Varanasi-221005, Uttar Pradesh, India
[b] Department of Physics, Institute of Science, Banaras Hindu University Varanasi- 221005, Uttar Pradesh, India
Department of Dairy Science & Food Technology, Institute of Science, Banaras Hindu University Varanasi-221005, Varanasi-221005, Uttar Pradesh, India

**e-mail: tripathi.csp@bhu.ac.in (C.S.P.T.), debanjan.chem@bhu.ac.in (D.G.)*

Experimental Section

Chemicals: Ferric Chloride hexahydrate ($FeCl_3.6H_2O$), Sodium Acetate (CH_3COONa), ethylene glycol ($C_2H_6O_2$), graphite flakes, Hydrogen peroxide (H_2O_2), Silver nitrate ($AgNO_3$), Potassium carbonate (K_2CO_3), and Ascorbic acid were brought from Merck Specialities Pvt. Ltd., Polyvinyl Pyrrolidone (PVP molecular weight ~ 40000), Phosphoric acid (H_3PO_4), Potassium permanganate ($KMnO_4$) were purchased from Loba Chemie Pvt. Lmt., Urea (NH_2CONH_2) was brought from Thermo Fisher Scientific India Pvt. Lmt., Sodium nitrite ($NaNO_2$) was purchased from Samir Tech Chem Pvt. Lmt., concentrated H_2SO_4 was brought from Himedia, Tannic acid was purchased from SRL Chem. All the solutions were prepared in distilled water. All the chemicals were used as provided without any further purification.

Instrumentations/ Characterization techniques: The X-ray diffraction measurements were carried out using XRD Bruker, Model-D8 Advance (Eco) to study the crystal structures of the as-synthesized nanocomposite. The X-ray photoelectron spectroscopy (XPS) measurements were carried out on PHI 5000 Versa Probe III spectrometer (ULVAC-PHI, Inc.) to investigate the elemental composition and oxidation state of metal nanoparticles present in the as synthesized nanocomposite. The surface morphology of the as-prepared Ag@Fe_3O_4-GO composite was observed by a scanning electron microscope (CARL ZEISS Model EVO-18) equipment. Elemental analysis of the Ag@Fe_3O_4-GO composite was done using Energy- Dispersive X-ray (EDX) detector (DS: 51N1000 – EDS System Company: Oxford Instruments Nanoanalysis) which was attached to the SEM machine. The morphology and size of the as-prepared nanocomposite were examined by using Transmission Electron Microscope (Model: Tecnai G2 20 TWIN Company: FEI Company of USA (S.E.A.) PTE, LTD). Magnetic properties of the as-prepared samples were determined using a

Vibrating Sample Magnetometer (MicroSense Easy VSM). Brunauer-Emmett-Teller (BET) experiment was performed on the QuantaChrome iQ2 instrument to evaluate the surface area and pore size. Raman spectra were recorded on a Renishaw inVia Raman microscope to observe structural alterations in the sample during the oxidation process. Fourier transform infrared spectroscopy (FT-IR) studies were conducted using the FTIR-4700 JASCO instrument at a resolution of 2cm-1. Atomic force microscopy (AFM) measurement was conducted using a multi-mode scanning probe microscope by NT-MDT Spectrum Instruments. The dynamic light scattering data was recorded to measure hydrodynamic size of Ag NPs on Malvern Panalytical Zetasizer Ultra (ZSU5700). The UV–vis absorption studies were conducted by a Fluorolog FL-3-11 Horiba Jobin-Yvon spectrophotometer.

Determination of Antimicrobial activity of Ag@Fe_3O_4-GO nanocomposite: Ag@Fe_3O_4-GO was tested for its ability to inhibit Gram-negative (*Escherichia coli* and *Salmonella enterica*) and Gram-positive (*Listeria ivanovii*) bacteria by modified Kirby-Bauer disk diffusion method (Bauer et al., 1966). Briefly, the pure bacterial cultures were propagated in Müller-Hinton broth at 35°C ± 2°C. A bacterial lawn of each test bacterial strain was prepared by overlaying melted cooled soft agar (8 mL) added with 50 µL fresh test bacterial strain having 10^6 colony-forming units (CFU)/mL on Müller-Hinton agar plates. As the agar solidified, 8 mm wells were punched into the Müller-Hinton agar plates by a sterile steel borer and sealed by adding 5-10 µL of molten agar (0.75% agar) to prevent leakage from the bottom of the wells. Ag@Fe_3O_4-GO nanocomposite was dissolved @ 50 mg/mL in sterile distilled water (stock suspension) and was serially diluted up to 528-fold to determine the minimum bactericidal concentration (MBC) of the nanocomposite. With help of a an autopipette, 100 µL of stock suspension and each dilution of the sample of nanoparticle suspension was poured onto each of wells in agar plates for all bacterial strains mentioned above. Gentamicin was taken as a positive control. Plates were incubated overnight at 35°C ± 2°C, the different levels of zone of inhibition were measured.

Supporting Information Figure 1. VSM of synthesized Fe_3O_4, Fe_3O_4-GO, 2% Ag@ Fe_3O_4-GO, and 5% Ag@ Fe_3O_4-GO samples

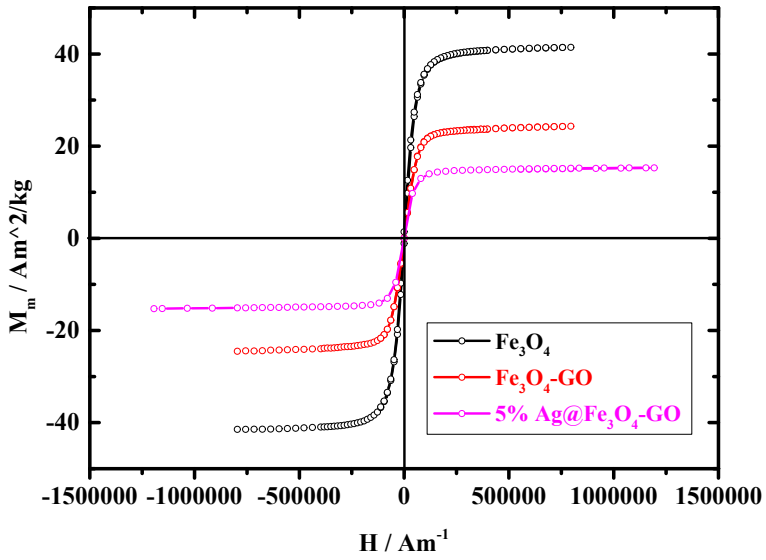

SI Figure 1: VSM of synthesized porous Fe_3O_4, Fe_3O_4-GO, 2% Ag@ Fe_3O_4-GO, and 5% Ag@ Fe_3O_4-GO samples

Supporting Information Figure 2. (a) and (b) represent the DLS and UV-visible spectra of synthesized Ag nanoparticles respectively. Figure 2 (b) inset visual picture of Ag nanoparticles.

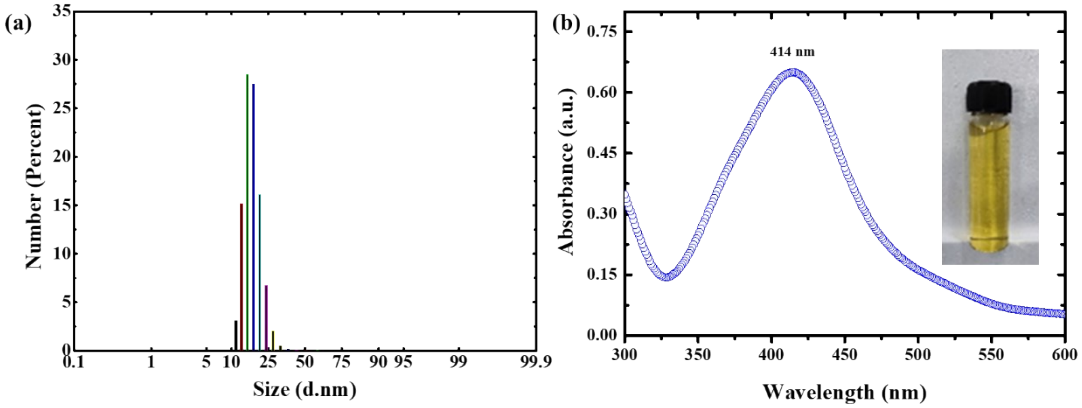

SI Figure 2. (a) and (b) represent the DLS and UV-Visible spectra of synthesized Ag nanoparticles respectively. Figure 2 (b) inset visual picture of Ag nanoparticles.

Supporting Information Figure 3 represents the N_2 adsorption-desorption isotherm of Ag@Fe_3O_4-GO NCs.

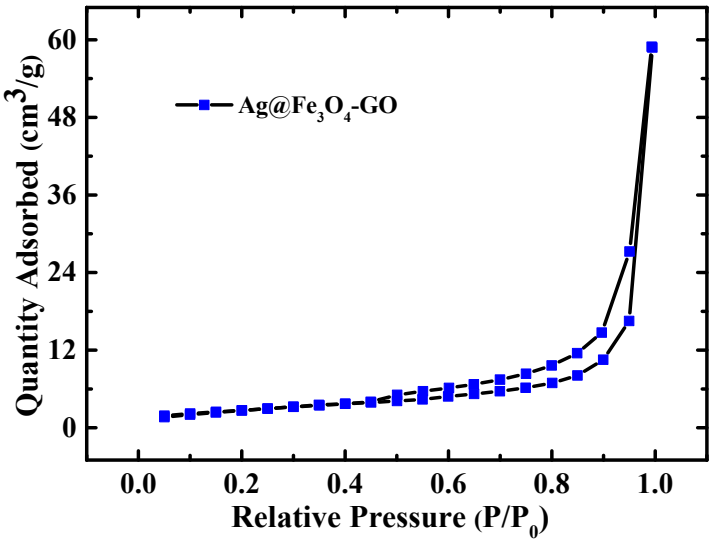

SI Figure 3. N_2 adsorption-desorption BET plot of Ag@Fe_3O_4-GO NCs.

Table 1: Concentration of Ag@Fe_3O_4-GO NCs vs clearance diameter (cm) data

		Diameter of Zone of clearance* (cm)		
Dilution	Concentration (mg/ml)	*Escherichia coli* (Gram-negative)	*Salmonella enterica* (Gram-negative)	*Listeria ivanovii* (Gram-positive)
1X	50	2.7±0.03	2.4±0.03	1.7±0.03
2X	25	2.5±0.03	2.2±0.02	1.7±0.03
4X	12.5	2.6±0.01	2.1±0.03	1.5±0.03
8X	6.25	2.7±0.03	2.0±0.03	1.5±0.06
16X	1.5625	2.2±0.03	1.9±0.03	1.4±0.09
32X	0.78125	2.0±0.03	1.7±0.03	1.3±0.07
64X	**0.390625**	**1.4±0.00**	1.5±0.03	1.3±0.03
132X	0.1953125	0.9±0.00	1.2±0.03	1.4±0.03
264X	**0.09765625**	0.9±0.00	**1.1±0.03**	1.4±0.07
528X	**0.048828125**	0.9±0.00	0.8±0.00	**1.3±0.06**
1056X	0.0244140625	0.8±0.00	0.8±0.00	0.8±0.00
	Gentamicin (32 mg/L)	3.2±0.03	3.6±0.03	1.9±0.03

*Zone of clearance more than 2mm is considered positive inhibitory activity. Zone of clearance calculated here includes the agar well diameter of 8mm

Table 2: Performance of the Ag@ Fe_3O_4-GO nanocomposites with existing materials.

S No	***Materials***	***Application***	***Ref***
01	*Ag@ Fe_3O_4-GO Nanocomposites*	Gaseous elemental mercury removal from coal-fired flue gas	*2*
02	Fe_3O_4/GO/Au-Ag nanocomposite	Organic molecule synthesis (spirooxindole-dihydropyridines)	*3*
03	Ag/ Fe_3O_4/RGO nanocomposites	(a) Reduction of organic pollutants (b) SERS detection	*4*
04	Fe3O4@ GO@ Ag@ PDA Composite	SERS detection of PAH	*5*
05	Ag-Fe3O4-graphene oxide	Electrochemical sensor	*6*
05	Ag@Fe_3O_4 nanoparticles decorated GO	(a) Photocatalytic (b) Supercapacitor (c) Antibacterial applications	*7*
06	Fe_3O_4/RGO Nanocomposite	Enhanced Photocatalytic Performance for Cr(VI) Reduction, Phenol Degradation, and Antibacterial Activity	*8*
07	***Ag@ Fe_3O_4-GO Nanocomposites***	***(a) SERS-based detection of organic dyes (methylene blue and methyl red)*** ***(b) Removal of oil and methylene blue from water.*** ***(c) Absorption and degradation of organic dyes and nitro aromatics.*** ***(d) Antibacterial activity.***	***Our Work***

References

1. Bauer, A.W., et al., 1966. Antibiotic Susceptibility Testing by a Standardized Single Disk Method. American Journal of Clinical Pathology, 45(4_ts): p. 493-496.

2. Ma, Y., Mu, B., Zhang, X., Xu, H., Qu, Z., Gao, L., Li, B. and Tian, J., 2019. Ag-Fe_3O_4@ rGO ternary magnetic adsorbent for gaseous elemental mercury removal from coal-fired flue gas. *Fuel*, *239*, pp.579-586.

3. Kavyani, S. and Baharfar, R., 2020. Design and characterization of Fe_3O_4/GO/Au-Ag nanocomposite as an efficient catalyst for the green synthesis of spirooxindole-dihydropyridines. *Applied Organometallic Chemistry*, *34*(4), p.e5560.

4. He, J., Song, G., Wang, X., Zhou, L. and Li, J., 2022. Multifunctional magnetic Fe_3O_4/GO/Ag composite microspheres for SERS detection and catalytic degradation of methylene blue and ciprofloxacin. *Journal of Alloys and Compounds*, *893*, p.162226.

5. Liu, J., Cui, W., Sang, S., Guan, L., Gu, K., Wang, Y. and Wang, J., 2022. Surface-Enhanced Raman Spectroscopic Investigation of PAHs at a Fe_3O_4@ GO@ Ag@ PDA Composite Substrates. Micromachines, 13(8), p.1253.

6. Li, B.Q., Nie, F., Sheng, Q.L. and Zheng, J.B., 2015. An electrochemical sensor for sensitive determination of nitrites based on Ag-Fe_3O_4-graphene oxide magnetic nanocomposites. *Chemical Papers*, *69*, pp.911-920.

7. Umar, A., Kumar, S.A., Inbanathan, S.S.R., Modarres, M., Kumar, R., Algadi, H., Ibrahim, A.A., Wendelbo, R., Packiaraj, R., Alhamami, M.A. and Baskoutas, S., 2022. Enhanced sunlight-driven photocatalytic, supercapacitor and antibacterial applications based on graphene oxide and magnetite-graphene oxide nanocomposites. *Ceramics International*, *48*(19), pp.29349-29358.

8. Padhi, D.K., Panigrahi, T.K., Parida, K., Singh, S.K. and Mishra, D.P., 2017. Green synthesis of Fe_3O_4/RGO nanocomposite with enhanced photocatalytic performance for Cr (VI) reduction, phenol degradation, and antibacterial activity. *ACS Sustainable Chemistry & Engineering*, *5*(11), pp.10551-10562.